Available online at www.sciencedirect.com
ScienceDirect

Journal of Solid State Chemistry 180 (2007) 2393–2399

JOURNAL OF SOLID STATE CHEMISTRY

www.elsevier.com/locate/jssc

High-temperature X-ray diffraction and specific heat studies on $GdAlO_3$, $Gd_3Al_5O_{12}$ and $Gd_4Al_2O_9$

Satyajeet Chaudhury[a,*], S.C. Parida[b], K.T. Pillai[a], K.D. Singh Mudher[a]

[a]*Fuel Chemistry Division, RC & I Group, Bhabha Atomic Research Centre, Trombay, Mumbai 400085, India*
[b]*Product Development Section, RC & I Group, Bhabha Atomic Research Centre, Trombay, Mumbai 400085, India*

Received 28 March 2007; received in revised form 23 May 2007; accepted 3 June 2007
Available online 8 June 2007

Abstract

Gadolinium aluminates, $GdAlO_3$, $Gd_3Al_5O_{12}$ and $Gd_4Al_2O_9$ were synthesized by the solution combustion method. Very fine particles in the nanoparticle range of ~10–20 nm could be prepared by this method as evidenced by surface area measurement by multipoint BET method. Thermal studies on these compounds were carried out using high-temperature X-ray diffraction (HT-XRD) and differential scanning calorimetry (DSC) methods. The thermal expansion coefficients of $GdAlO_3$, $Gd_3Al_5O_{12}$ and $Gd_4Al_2O_9$ were calculated from the lattice parameter data and specific heats were calculated from DSC data. The lattice parameters of $GdAlO_3$ and $Gd_3Al_5O_{12}$ were found to increase linearly with temperature whereas $Gd_4Al_2O_9$ did not show a linear trend. The specific heats of these compounds show an increasing trend with increase in aluminum atom fraction. Based on the thermodynamic data available in the literature and the specific heat data obtained in this study, oxygen potential diagram was constructed at 1000 K.

Keywords: Gadolinium aluminate; Solution combustion; Thermal studies; HT-XRD; DSC; Nanoparticle

---

1. Introduction

Solid solutions of UO_2–RE_2O_3 (where RE = Sm, Eu, Gd and Er) are being considered as potential fuel pellets whereas lanthanide sesquioxide acts as a burnable poison to suppress initial excess reactivity at the beginning of life in nuclear reactors [1–3]. Among the sesquioxides, Gd_2O_3 is being used commonly worldwide. Gadolinium aluminate is currently under development as candidate material for neutron absorption and control rod applications [4]. Information on thermal expansion coefficient, specific heat, thermal conductivity, etc. of such materials as a function of temperature is essential to evaluate the thermophysical properties under temperature gradients. As a part of the work program for the development of rare-earth-based materials of interest in nuclear technology, thermal studies were carried out on selected compounds of the Gd–Al–O system.

In the pseudo-binary system Gd_2O_3–Al_2O_3, two stable compounds, $Gd_4Al_2O_9$ and $GdAlO_3$ (mole ratios Gd_2O_3:Al_2O_3 = 2:1 and 1:1, respectively), are known [5–8]. $Gd_4Al_2O_9$ is monoclinic and its structure is related to that of the mineral cuspidine, $Ca_4Si_2O_7F_2$. At 1406 K, $Gd_4Al_2O_9$ undergoes a reversible, possibly martenstic phase transformation [9] as do all other $RE_4Al_2O_9$ phases at specific temperatures between 1273 and 1673 K, followed by congruent melting at 2224 K. $GdAlO_3$ crystallizes in an orthorhombic perovskite-type structure and melts congruently at 2342 K. Two other gadolinium aluminates, $Gd_3Al_5O_{12}$ and $GdAl_{11}O_{18}$ (mole ratios Gd_2O_3:Al_2O_3 = 3:5 and 1:11, respectively), have been reported in the literature [10–14], but their thermodynamic stability has not been thoroughly clarified. $Gd_3Al_5O_{12}$ belongs to the garnet structure type. It has been reported that $Gd_3Al_5O_{12}$ on heat treatment at 1773 K for 24 h undergoes complete decomposition to $GdAlO_3$ and Al_2O_3 [15]. $GdAl_{11}O_{18}$ has magnetoplumbite-type structure. It is stable only at higher temperatures (> 1773 K) and eutectically decomposes to $GdAlO_3$ and Al_2O_3 at lower temperatures [15].

The aim of the present work, therefore, was to synthesize the three most stable compounds $GdAlO_3$, $Gd_3Al_5O_{12}$ and

---

*Corresponding author. Fax: +91 22 2550 5151.
E-mail address: saty@apsara.barc.ernet.in (S. Chaudhury).

0022-4596/$ - see front matter © 2007 Elsevier Inc. All rights reserved.
doi:10.1016/j.jssc.2007.06.003

$Gd_4Al_2O_9$ by solution combustion method and to investigate their thermal expansion behavior and specific heat as a function of temperature.

2. Experimental

Synthetic compounds of $GdAlO_3$, $Gd_3Al_5O_{12}$ and $Gd_4Al_2O_9$ were prepared by taking stochiometric amounts of gadolinium nitrate, $Gd(NO_3)_3$ (A.R. grade) and aluminum nitrate, $Al(NO_3)_3$ (A.R. grade) and mixing with glycerol. The mixtures were heated on a hot plate with continuous stirring until a brown fine powder (precursor) was formed. The precursor powders were calcined at 1023 K for 16 h to get crystalline phases of $GdAlO_3$, $Gd_3Al_5O_{12}$ and $Gd_4Al_2O_9$. The formation of the compounds was examined by X-ray powder diffraction (XRD) method. High-temperature XRD patterns of these compounds were recorded under reduced pressure ($\sim 10^{-5}$ mbar) in a STOE diffractometer from 298 to 1273 K. The patterns were taken at an interval of 100 K with Cu$K\alpha$-radiation ($\lambda = 1.5406$ Å) in the range $2\theta = 10$–65° using HDK-2.4 Buhler high-temperature attachment. In the high-temperature chamber, the well-ground samples, mixed with a drop of collodine were mounted on a platinum–rhodium sample carrier which is spot welded at the bottom with a Pt/Pt–13%Rh thermocouple and was resistively heated at a programmed rate. The sample temperature was controlled by a PID temperature controller within ± 1 K. The sample was kept isothermal for about 60 min at each temperature step in order to ensure thermal equilibrium. The unit cell parameters at each temperature were determined using least-squares method using a computer program by Wadhawan [16] with an accuracy of ± 0.001 Å.

Surface area of these compounds was measured by multipoint BET method using Sorptomatic-1990, CE Instruments, Italy.

Specific heats of these compounds were measured using a heat flux type differential scanning calorimeter (DSC 131, SETARAM Instrumentations, France). Temperature calibration, heat calibration and procedure for specific heat measurement using this calorimeter is extensively discussed in an earlier publication [17]. The classical three-step method with continuous heating mode was followed in this study to measure the specific heat. NIST synthetic sapphire (SRM-720) in the powder form was used as the reference material. The specific heat of the sample under investigation can be calculated by a simple comparison of the heat flow rates into the sample and into the calibration substance as illustrated in the literature [17]. The expression used for the calculation of specific heat of the sample is given as

$$C_p(T)_{\text{Sample}} = \frac{\text{HF}_{\text{Sample}} - \text{HF}_{\text{Blank}}}{\text{HF}_{\text{Ref}} - \text{HF}_{\text{Blank}}} \times \frac{M_{\text{Ref}}}{M_{\text{Sample}}} \times C_p(T)_{\text{Ref}}, \tag{1}$$

where HF_{Blank}, HF_{Ref} and $\text{HF}_{\text{Sample}}$ represent heat flow during blank, reference and sample steps, respectively. $C_p(T)_{\text{Sample}}$ and $C_p(T)_{\text{Ref}}$ represent the specific heats of sample and reference material, whereas M_{Sample} and M_{Ref} represent the masses of sample and reference, respectively. Accuracy of the measurements was checked by measuring the specific heat of Fe_2O_3 (mass fraction 0.998) in the temperature range from 300 to 860 K and the values were found to be within $\pm 2\%$ compared with the literature values [18].

3. Results and discussion

$GdAlO_3$ (orthorhombic perovskite-type structure and S.G.: *Pbnm* (62)). $Gd_3Al_5O_{12}$ (cubic garnet-type structure and S.G.: *Ia*3*d* (230)) and $Gd_4Al_2O_9$ (monoclinic structure and S.G.: $P2_1/c$) could be prepared by solution combustion (SC) synthesis method in the presence of glycerol. Glycerol acts as a fuel and serves two purposes:

(a) It is a source of C and H, which on combustion form CO_2 and H_2O and liberates heat.
(b) It forms complexes with the metal ions facilitating homogeneous mixing of the cations in solution.

The basic reactions involved with glycerol could be

$$M(NO_3)_3 + 3H_2O \rightarrow M(OH)_3 + 3HNO_3, \tag{2}$$

$$2HNO_3 \rightarrow H_2O + 2NO + 3[O], \tag{3}$$

$$C_3H_8O_3 + 7[O] \rightarrow 3CO_2 + 4H_2O, \tag{4}$$

where M stands for gadolinium and aluminum. The overall reaction can be written as

$$14M(NO_3)_3 + 9C_3H_8O_3 \rightarrow 14M(OH)_3 + 42\,NO + 27\,CO_2 + 15\,H_2O. \tag{5}$$

In reality, the reactions seem to be more complicated. Glycerol seems to decompose to form, among other products, carboxylic acids, which in turn, form complexes with metal ions, thereby preventing the precipitation of aluminum at lower pH. This is probably the reason for simultaneous precipitation of aluminum and gadolinium at a higher pH of around 7. The high viscosity of glycerol may also be playing a role in preventing the segregation of aluminum and gadolinium during precipitation. The exothermicity (adiabatic temperature, T_{ad}) of the redox reaction is very high. Though these aspects are not fully understood, the usefulness of the 'glycerol route' for obtaining good-quality gadolinium aluminate powder has been established. Potential advantages of this wet chemical route over the conventional solid state reaction method include better homogeneity, better compositional control and lower processing temperatures. The surface area found out by multipoint BET method for $GdAlO_3$, $Gd_3Al_5O_{12}$ and $Gd_4Al_2O_9$ were 56.4, 56.26 and 57.50 m^2/g, respectively. Pore volume of the above samples was found to be negligible indicating non-porous nature of the particles. Particle size calculated from surface area ($d = 6/\rho a$, where d is the diameter, ρ the density and a the surface area) were 14.3, 17.87 and 18.56 nm for $GdAlO_3$, $Gd_3Al_5O_{12}$ and $Gd_4Al_2O_9$, respectively.

The XRD patterns of $GdAlO_3$, $Gd_3Al_5O_{12}$ and $Gd_4Al_2O_9$ prepared by solution combustion method shown in Fig. 1 were compared with reported data [19] which confirmed their formation. The unit cell parameters of these compounds at room temperature were determined using least-squares refinement program [16] and are shown in Table 1.

3.1. Thermal expansion behavior

The HT-XRD patterns of $GdAlO_3$, $Gd_3Al_5O_{12}$ and $Gd_4Al_2O_9$ recorded at different temperatures upto 1273 K did not show any phase change except for the shift in the X-ray line positions to lower values of 2θ showing expansion of the unit cell. The lattice parameters were obtained within an accuracy of ± 0.001 Å using least-squares refinement method. The variation of lattice parameters of $GdAlO_3$, $Gd_3Al_5O_{12}$ and $Gd_4Al_2O_9$ with temperature is shown in Figs. 2–4, respectively. The lattice parameters are best fitted to linear expressions for $GdAlO_3$ and $Gd_3Al_5O_{12}$ by Eqs. (6)–(11) but for $Gd_4Al_2O_9$, the parameters are best fitted to third-order polynomial expressions related by Eqs. (12)–(15), given below.

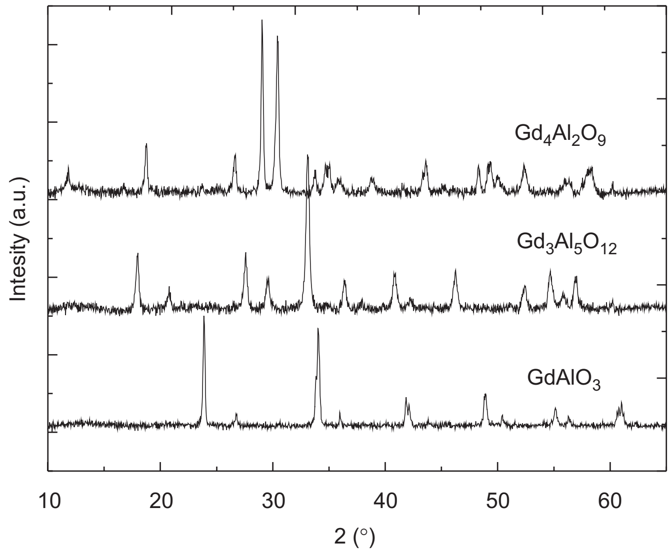

Fig. 1. Room-temperature X-ray diffraction patterns of $GdAlO_3$, $Gd_3Al_5O_{12}$ and $Gd_4Al_2O_9$.

For $GdAlO_3$

$$a_T\,(\text{Å}) = 5.230 + 6.422 \times 10^{-5}\,T\,(\text{K}), \quad (6)$$

$$b_T\,(\text{Å}) = 5.289 + 3.110 \times 10^{-5}\,T\,(\text{K}), \quad (7)$$

$$c_T\,(\text{Å}) = 7.415 + 8.491 \times 10^{-5}\,T\,(\text{K}), \quad (8)$$

$$V_T\,(\text{Å}^3) = 205.030 + 6.220 \times 10^{-3}\,T\,(\text{K}). \quad (9)$$

For $Gd_3Al_5O_{12}$

$$a_T\,(\text{Å}) = 12.074 + 1.121 \times 10^{-4}\,T\,(\text{K}), \quad (10)$$

$$V_T\,(\text{Å}^3) = 1759.538 + 5.020 \times 10^{-2}\,T\,(\text{K}), \quad (11)$$

For $Gd_4Al_2O_9$

$$a_T\,(\text{Å}) = 11.209 + 1.734 \times 10^{-4}\,T\,(\text{K}) - 2.035 \times 10^{-7}\,T^2\,(\text{K}) + 9.895 \times 10^{-11}\,T^3\,(\text{K}), \quad (12)$$

$$b_T\,(\text{Å}) = 10.701 - 1.906 \times 10^{-4}\,T\,(\text{K}) + 4.866 \times 10^{-7}\,T^2\,(\text{K}) - 2.505 \times 10^{-10}\,T^3\,(\text{K}), \quad (13)$$

$$c_T\,(\text{Å}) = 7.559 + 3.516 \times 10^{-6}\,T\,(\text{K}) + 4.249 \times 10^{-8}\,T^2\,(\text{K}) - 1.316 \times 10^{-11}\,T^3\,(\text{K}), \quad (14)$$

$$V_T\,(\text{Å}^3) = 855.299 + 3.300 \times 10^{-3}\,T\,(\text{K}) + 2.189 \times 10^{-5}\,T^2\,(\text{K}) - 1.165 \times 10^{-8}\,T^3\,(\text{K}). \quad (15)$$

These expressions show that the lattice parameters of $GdAlO_3$ and $Gd_3Al_5O_{12}$ increase linearly with temperature between 298 and 1273 K, whereas $Gd_4Al_2O_9$ do not show linear trend. The values of linear thermal expansion coefficient (α_T) at any temperature (T/K) were calculated using the following relation:

$$\text{Thermal expansion coefficient, } \alpha_T = \frac{\delta a}{\delta T} \times \frac{1}{a_{298}}, \quad (16)$$

where δa is the change in lattice parameter corresponding to a change in temperature δT and a_{298} is the lattice parameter at 298 K. Average thermal expansion coefficient of $GdAlO_3$, $Gd_3Al_5O_{12}$ and $Gd_4Al_2O_9$ were theoretically

Table 1
Lattice parameters refined from room-temperature X-ray powder diffraction data

Compound	Structure	a (Å)	b (Å)	c (Å)	β (deg)	Z	V (Å^3)
$GdAlO_3$	Orthorhombic	5.247(2)	5.299(1)	7.438(2)		4	206.8(1)
$Gd_3Al_5O_{12}$	Cubic	12.108(2)				8	1775.1(3)
$Gd_4Al_2O_9$	Monoclinic	11.246(2)	10.679(6)	7.563(2)	109.2(2)	4	857.8(5)

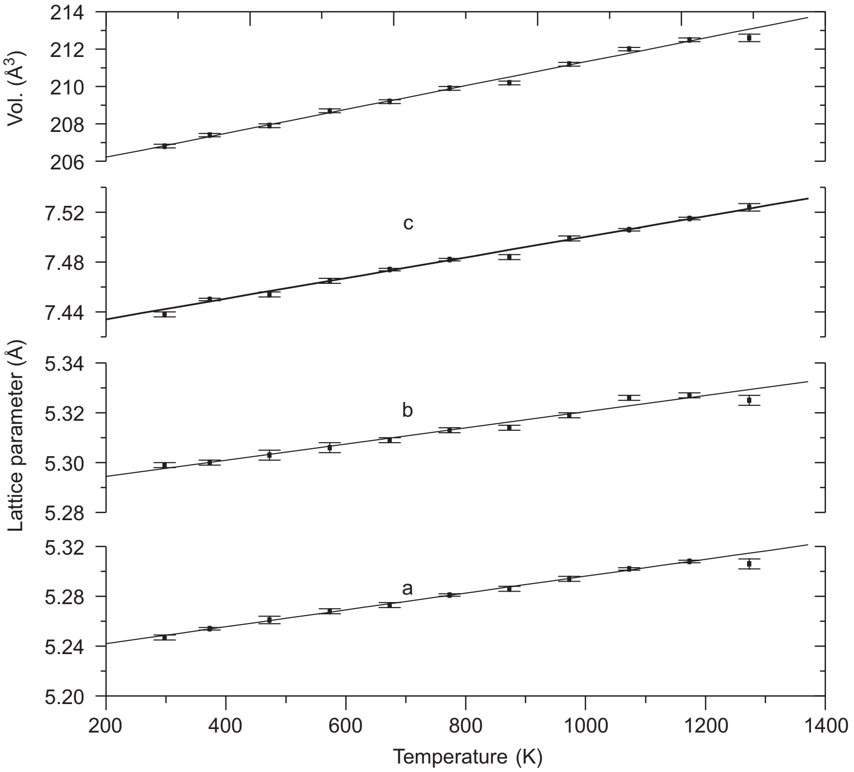

Fig. 2. Variation of lattice parameters with temperature for $GdAlO_3$.

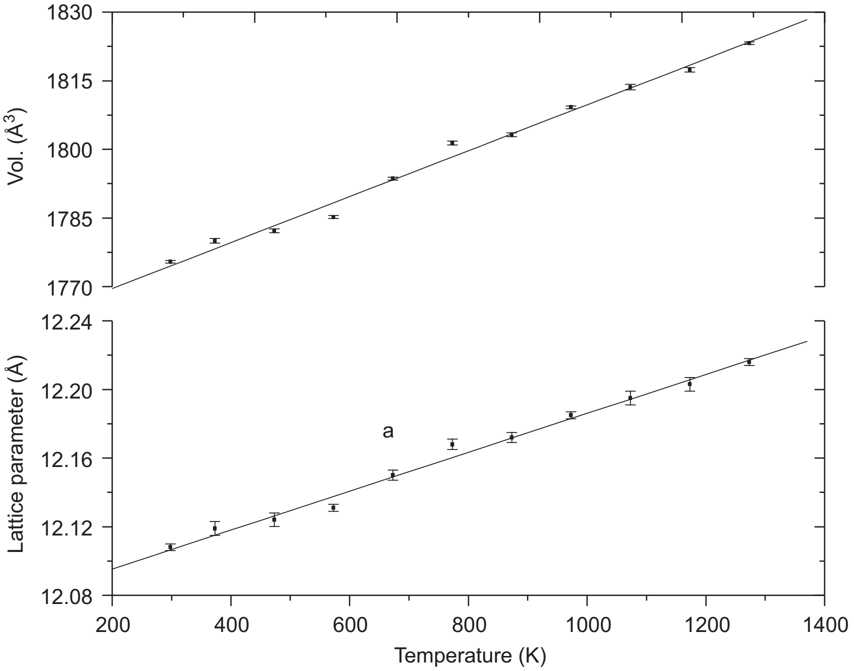

Fig. 3. Variation of lattice parameters with temperature for $Gd_3Al_5O_{12}$.

calculated from the lattice parameter values by using Eq. (16) and the values are given in Table 2. The values of average thermal expansion coefficient in the present study are close to the value of ceramic materials like UO_2 ($\alpha_a = 10.47 \times 10^{-6}\,K^{-1}$) [20] and ThO_2 ($\alpha_a = 9.04 \times 10^{-6}\,K^{-1}$) [21].

3.2. Specific heat measurements

Experimental values of specific heats of these compounds are not reported in the literature. However, the estimated values of these compounds are reported in the literature [8,18]. The specific heats of the compounds as a

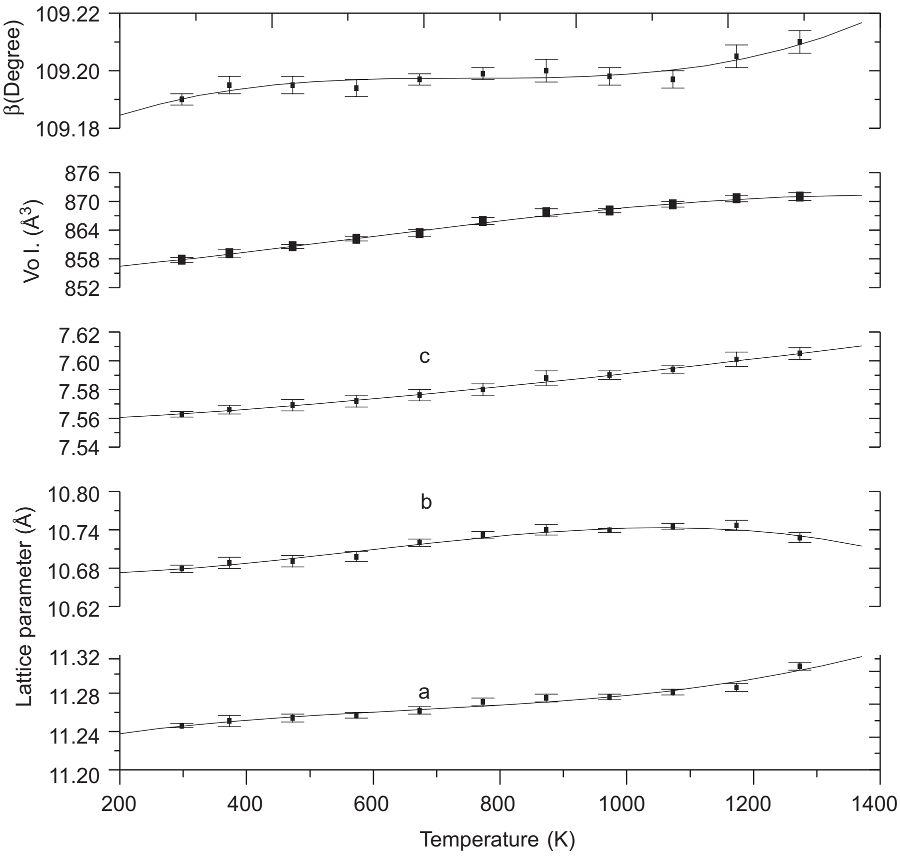

Fig. 4. Variation of lattice parameters with temperature for $Gd_4Al_2O_9$.

Table 2
Average thermal expansion coefficient of compounds in the temperature range 298–1273 K

Compound	Average thermal expansion coefficient · (10^6) (K^{-1})			
	α_a	α_b	α_c	α_v
$GdAlO_3$	13.8	5.04	13.1	31.8
$Gd_3Al_5O_{12}$	9.23			27.2
$Gd_4Al_2O_9$	4.42	8.30	5.12	18.4

function of temperature are best fitted by the least-squares method into the following expressions:

For the compound $GdAlO_3$,

$$C_p^0\,(\mathrm{J\,g^{-1}\,K^{-1}})\,(\pm 2.0\%) = 0.48827 + 0.00009T\,(\mathrm{K}) - 9409.88T^2\,(\mathrm{K}). \tag{17}$$

For the compound $Gd_3Al_5O_{12}$,

$$C_p^0\,(\mathrm{J\,g^{-1}\,K^{-1}})\,(\pm 2.0\%) = 0.61195 + 0.00005T\,(\mathrm{K}) - 15374.42T^2\,(\mathrm{K}). \tag{18}$$

For the compound $Gd_4Al_2O_9$,

$$C_p^0\,(\mathrm{J\,g^{-1}\,K^{-1}})\,(\pm 2.0\%) = 0.45853 + 0.00004T\,(\mathrm{K}) - 9834.53T^2\,(\mathrm{K}). \tag{19}$$

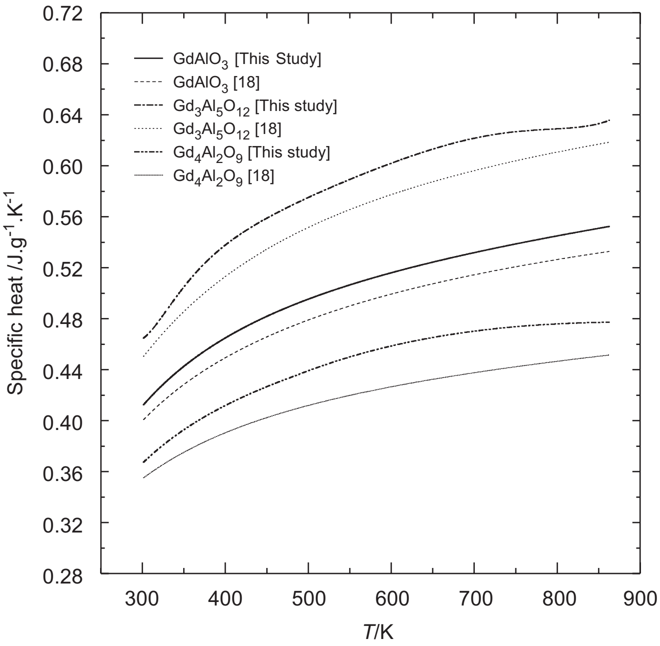

Fig. 5. Comparison of experimental and estimated specific heats of $GdAlO_3$, $Gd_3Al_5O_{12}$ and $Gd_4Al_2O_9$.

These experimental specific heat capacities are compared with those reported in the literature [18] and are shown in Fig. 5. It can be seen from the figure that the specific heats obtained in this study are higher than the values taken from Ref. [18]. This discrepancy could not be explained unless a third set of specific heat capacity data is available.

It can be inferred from the comparison plot that the specific heats of these compounds follow the trend: specific heat ($Gd_3Al_5O_{12}$) > specific heat ($GdAlO_3$) > specific heat ($Gd_4Al_2O_9$). This trend is in order with the atom fraction of aluminum for these compounds: $Gd_3Al_5O_{12}$ (atom fraction Al = 0.25) > $GdAlO_3$ (atom fraction Al = 0.20) > $Gd_4Al_2O_9$ (atom fraction Al = 0.133). It is imperative to mention here that a complete data set from very low temperature (near zero) to high temperature (above 1000 K) is required in order to explain this trend by formulating suitable thermodynamic models.

Based on the available estimated thermodynamic data reported in the literature [8] and the specific heat data obtained in the present study, the standard molar Gibbs energies of formation ($\Delta_f G^o_m$) of these ternary oxides have been calculated by second law method at 1000 K. For this calculation, the specific heats for all these compounds measured in this study in the temperature range 300–850 K have been extrapolated to 1000 K assuming absence of any phase transition in all the three compounds $GdAlO_3$, $Gd_3Al_5O_{12}$ and $Gd_4Al_2O_9$. The oxygen chemical potentials corresponding to various equilibrium reactions in the system Gd–Al–O have been calculated at 1000 K using the calculated values of $\Delta_f G^o_m$ of different phases. In the ternary system containing two metallic elements (Gd and Al) and one gas phase (O_2), it is interesting to observe the change in phase relations by changing the activity of gas phase. In generalized oxygen potential diagram, the values of oxygen potentials are plotted against the composition parameter which is generally the cationic fraction. The oxygen potential diagram for the system Gd–Al–O constructed in this study is shown in Fig. 6. The composition parameter is defined as $\eta_{Gd}/(\eta_{Gd}+\eta_{Al})$. The alloy–oxide equilibria are not shown in the figure because thermodynamic data for Gd–Al alloys are not available. It is evident from the diagram that these ternary oxides are stable at 1000 K at oxygen potentials far below that prevailing over the two phases: Al (Liq.) + Al_2O_3 (s). It is also apparent from the diagram that on gradually decreasing the oxygen partial pressure at 1000 K, the compound $Gd_3Al_5O_{12}$ will decompose to $GdAlO_3$ and Al (Liq.), $GdAlO_3$ will decompose to $Gd_4Al_2O_9$ and Al (Liq.) and $Gd_4Al_2O_9$ will decompose to Gd_2O_3 and Al. (Liq.). Similar diagrams can be constructed at other temperature of interest which aids valuable information on phase stability.

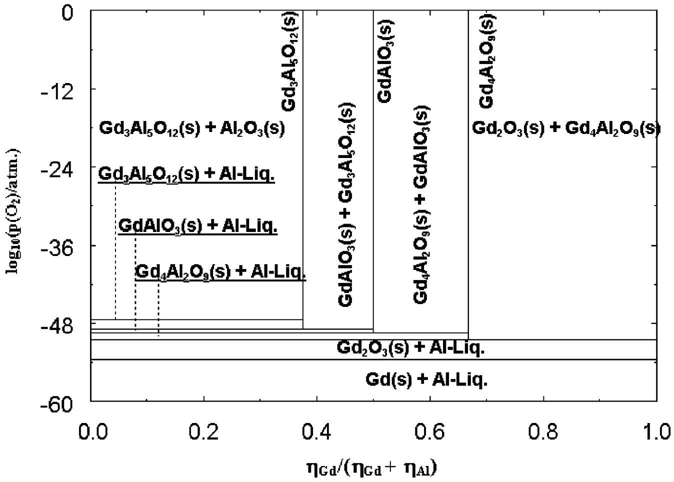

Fig. 6. Isothermal oxygen potential diagram for the system Gd–Al–O at 1000 K.

4. Conclusion

Synthetic samples of $GdAlO_3$, $Gd_3Al_5O_{12}$ and $Gd_4Al_2O_9$ were synthesized by solution combustion route. Particle size found out from surface area was in nanoparticle range of 10–20 nm. Thermal expansion behavior of these samples was studied by HT-XRD method. The lattice parameters of $GdAlO_3$ and $Gd_3Al_5O_{12}$ were found to increase linearly with temperature whereas $Gd_4Al_2O_9$ did not show a linear trend. Specific heats were measured by DSC. The specific heats of these compounds showed increasing trend with increase in atom fraction of aluminum. Isothermal oxygen potential diagram was constructed at 1000 K, which reveals that on gradually decreasing the oxygen partial pressure, the compound $Gd_3Al_5O_{12}$ will decompose to $GdAlO_3$ and Al (Liq.), $GdAlO_3$ will decompose to $Gd_4Al_2O_9$ and Al (Liq.) and $Gd_4Al_2O_9$ will decompose to Gd_2O_3 and Al. (Liq.).

Acknowledgments

The authors are thankful to Dr. V. Venugopal, Director, Radiochemistry & Isotope Group and Dr. S.K. Aggarwal, Head, Fuel Chemistry Division, for their keen interest and encouragement in this work.

References

[1] H. Bairiot, P. Deramaix, C. Vandenburg, Improved utilization of water reactor fuel, with special emphasis on extended burn ups and plutonium recycling, in: Proceedings of the Special IAEA Meeting, Report Conference 8405285, 1984, p. 86.

[2] H. Assmann, J.P. Robin, Guidebook on quality control of mixed oxides and gadolinium bearing fuels for light water reactors, IAEA-TECDOC-584, IAEA, Vienna, 1983, p. 51.

[3] K.W. Song, K.S. Kim, J.H. Yang, K.W. Kang, Y.H. Jung, J. Nucl. Mater. 288 (2001) 92.

[4] S. Girija, G. Seenivasan, M.V. Krishnaiah, P. Srirama Murti, J. Nucl. Mater. 249 (1997) 259.

[5] P.P. Budnikov, V.I. Kushakovski, V.S. Belenvantsev, Dokl. Akad. Nauk. SSSR 165 (1965) 1057 (in Russian). Summarised in English by N.A. Toropov, V.P. Barzakovskii, V.V. Lapin, N.N. Kurtseva, Handbook of Phase Diagrams of Silicate Systems, vol. 1; Binary Systems, vol. 2, Metal–Oxygen Compounds in Silicate Systems, Israel Program for Scientific Transactions Ltd., Jerusalem, 1972.

[6] M. Mizuno, T. Yamada, T. Noguchi, Yogyo-Kyoki Shi 85 (1977) 543 (in Japanese).

[7] M. Mizuno, T. Yamada, Nagoya-Kogyo Gijutsu Shikensho Hokoku 39 (1990) 156 (in Japanese).

[8] P. Wu, A.P. Pelton, J. Alloys Compds. 179 (1992) 259.

[9] H. Yamane, K. Ogawara, M. Omori, T. Hirai, J. Am. Ceram. Soc. 78 (1995) 2385.

[10] F. Bertaut, F. Forrat, C.R. Acad. Sci., Ser. B 243 (1956) 1219 (in French).

[11] F. Euler, J.A. Bruce, Acta Crystallogr. 19 (1965) 971.

[12] T. Shishido, K. Okamura, S. Yajima, J. Am. Ceram. Soc. 61 (1978) 373.

[13] T. Shishido, J. Mater. Sci. 14 (1979) 823.

[14] N.N. Matyushenko, E.P. Shevyakova, E.V. Lifshits, V.N. Lapina, Russ. J. Inorg. Chem. 30 (1985) 942.

[15] K. Kolitsch, H.J. Seifert, F. Aldinger, J. Alloys Compds. 257 (1997) 104.

[16] V.K. Wadhawan, LATPAR, A Least Squares Fitting Program, Neutron Physics Division, Bhabha Atomic Research Centre, Mumbai, India, Private Communication.

[17] S.C. Parida, S.K. Rakshit, S. Dash, Z. Singh, R. Prasad, V. Venugopal, J. Chem. Thermodyn. 36 (2004) 911.

[18] FactSage, Version 5.3.1, Thermfact Database, GTT-Technologies GmbH, Germany, 1976–2004.

[19] International Centre for Diffraction Data, Newton Square, PA, USA. PDF No. 46–395 ($GdAlO_3$), 32–383 ($Gd_3Al_5O_{12}$) and 46–396 ($Gd_4Al_2O_9$).

[20] K.H. Kang, H.J. Ryu, K.C. Song, M.S. Yang, J. Nucl. Mater. 301 (2002) 242.

[21] A.K. Tyagi, M.D. Mathews, B.R. Ambekar, R. Ramchandran, Thermochem. Acta 421 (2004) 69.